Electronic Supplementary Material (ESI) for Soft Matter.

Orthogonal Superposition Dielectric Rheometry (OSDR):

Noah H. Cho[a], Jiachun Shi[c], Ryan P. Murphy[d], John K. Riley[b], Simon Rogers[c], Jeffrey J. Richards[a]

[a]Department of Chemical & Biological Engineering, Northwestern University, Evanston, IL, USA

[b]Performance Materials & Coatings, The Dow Chemical Company, Collegeville, Pennsylvania, USA

[c]Department of Chemical and Biomolecular Engineering, University of Illinois of Urbana-Champaign, Urbana, Illinois

[d]NIST Center for Neutron Research, National Institute of Standards and Technology, Gaithersburg, MD, USA

S.1. Linear viscoelasticity measurements as a function of water content in reverse WLMs

Small amplitude oscillatory shear (SAOS) was conducted as a function of water content, W = $[H_2O]/[Lec]$ = 2.0 – 3.2 at fixed concentration of lecithin micelle, 50mg/ml, and temperature, 25°C. Each experiment was performed using a stress-contrilled rheometer (Ares G2, TA Instruments) with a cone and plate geometry (D = 40 mm and cone angle = 1°) with well-controlled temperature using petier system within ± 0.1 °C. At each water content, the storage and loss modulus was determined as a function of frequency, ω, from 0.01 to 100 rad/s with fixed strain, γ_0 = 0.01. We found that there are well-defined crossover of storage and loss modulus at crossover frequency,

ω_c. The representative mechanical spectra at water content, W = 2.4 and 3.0, was plotted in Figure S1.

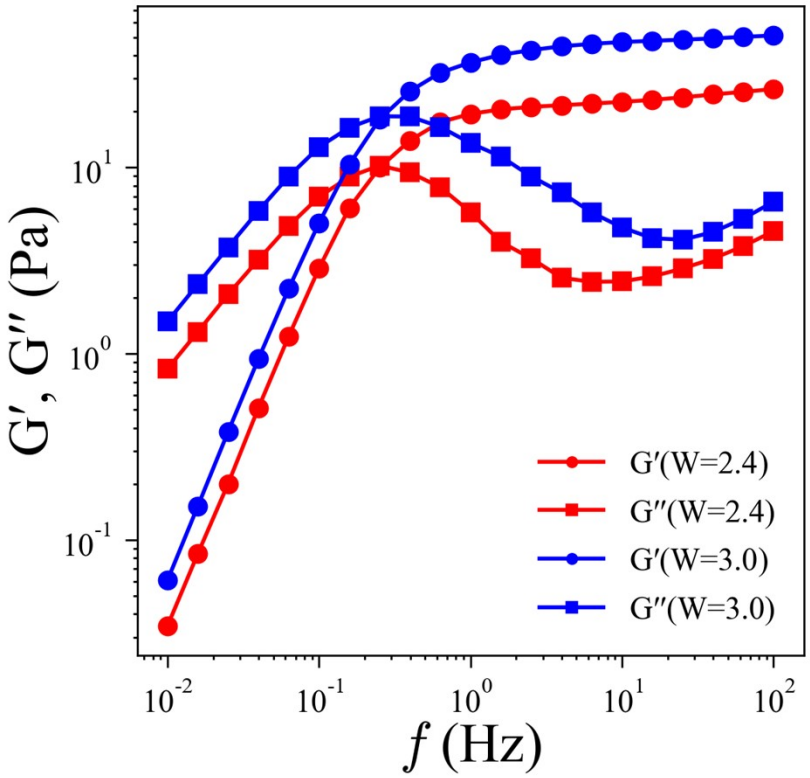

Figure S1. Linear viscoelasticity measurements of two different W = 2.4 (unbranched, red) and 3.0 (branched, blue) solutions in the function of frequency. Storage modulus was plotted with circle markers (●) and loss modulus was drawn with square markers (■).

From the crossover frequency, we estimated the primary relaxation time as $\tau_R = 1/\omega_c$. The zero-shear viscosity was calculated with $\eta_0 = \lim_{\omega \to 0} \sqrt{G' + G''}/\omega$ when the storage and loss modulus followed low-frequency terminal scaling, $G'' \sim \omega$ and $G' \sim \omega^2$. The plateau modulus, G_p, was

calculated from $G_p = \eta_0/\tau_R$. All linear viscoelastic parameters are represented in Figure S2 as the function of water fraction. Table S1 summarized the values of rheological parameters.

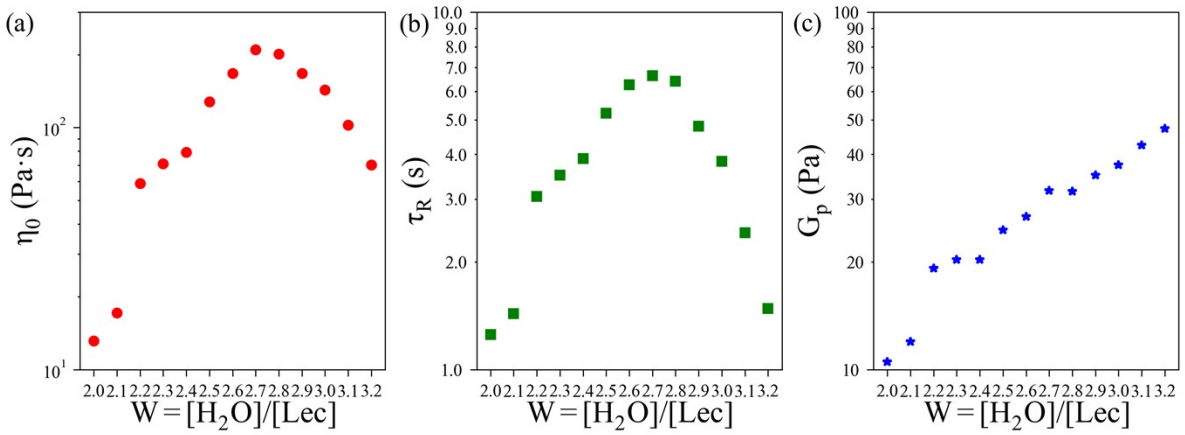

Figure S2. (a) Viscosity, (b) relaation time, (c) plateau modulus measurements as a function of water content, W, in 50 mg/ml lecithin concentration.

W	η_0 (Pa·s)	τ_R (s)	G_p (Pa)
2.0	13.2	1.25	10.5
2.1	17.2	1.44	12.0
2.2	58.7	3.05	19.2
2.3	70.9	3.50	20.3
2.4	79.1	3.89	20.3
2.5	128.0	5.21	24.6
2.6	167.9	6.26	26.8
2.7	210.2	6.64	31.7
2.8	201.7	6.40	31.5
2.9	167.8	4.80	35.0

3.0	143.2	3.83	37.4
3.1	102.4	2.41	42.5
3.2	70.1	1.48	47.2

Table 1. Summary of rheology data as a function of water fraction, W, at 50 mg/ml WLM solutions.

S.2. Dielectric spectra of unbranched and branched WLMs at a quiescent state.

Using dielectric spectroscopy, we premeasured the dielectric response of an unbranched (W = 2.4) and branched (W = 3.0) WLMs at constant concentration, 50mg/ml. The dielectric spectra was corrected from independent measurements of short ciruit current and capacitance of the empty cell. The accessible frequency, *f*, range of dielectric measurements was from 20 Hz to 50 MHz. The complex dielectric permittivity was represented with real component, ε', which is dielectric constant and imaginary component, ε'', which is dielectric loss. The dielectric responses were plotted in Figure S3 with unbranched and branched WLMs.

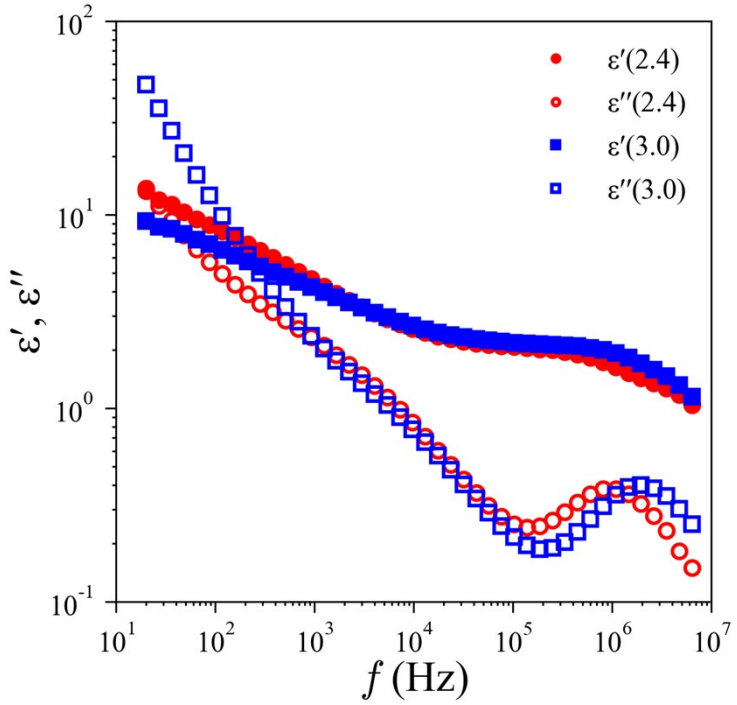

Figure S3. Dielectric spectra of two different topology from unbranched to branched WLMs as a function of frequency. Dielectric constant, $\varepsilon^{'}$, was plotted with solid markers and dielectric loss, $\varepsilon^{''}$, was drawn with hollow makres.

S.3. Dielectric rheology spectra as a function of Wi number between unbranched and branched WLMs.

We perfomed rheo-dielectric measurements on both unrbranched and branched WLMs at rest and under shear rate, $\dot{\gamma}$, following the protocol developed by Riley et al. The strain-controlled rheometer (Ares G2, TA instruments) equipped with a customized stainless-steel Couette geometry under same configuration of geometry. With careful treatments of an evaporation of decane and water, we measured the stress responses and simultaneously the dielectric responses

as a function of shear rate. The shear rate was converted to Weissenber number given as $Wi = \tau_R \dot{\gamma}$ to compare the unbranched and branched WLMs. Summary of dielectric reponses as the function of Wi was plotted in Figure S4.

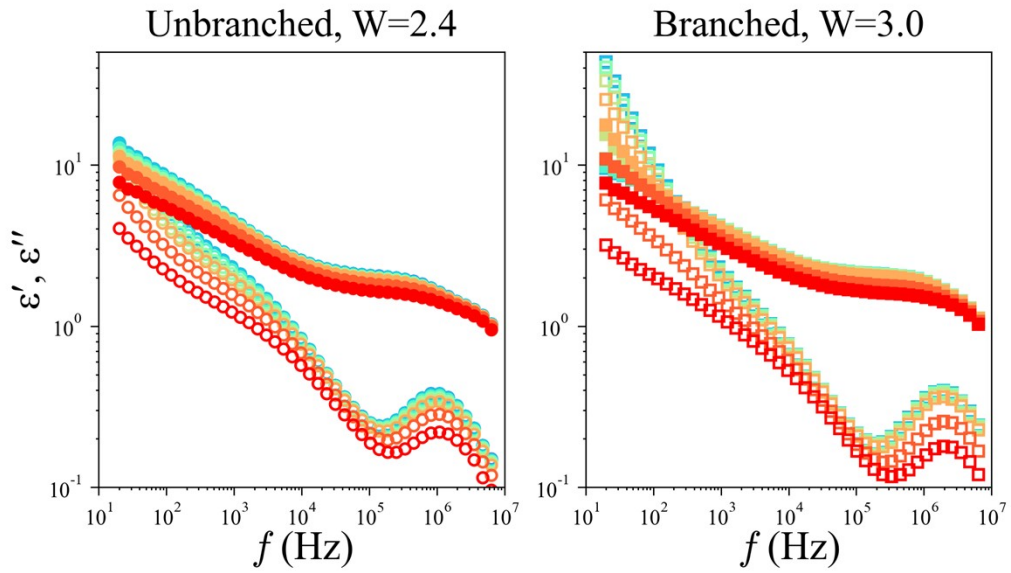

Figure S4. Dielectric spectra as a function of frequency and Wi number between unbranched and branched WLM solutions.

S.4. Representative 2D SANS patterns in 1-3 plane in steady state on both unbranched and branched WLMs.

Compared to the established Rheo-dielectric technique under flow, the simulataneous measurements of the 2D scattering patterns of very small angle neutron scattering explained in Material and Method section in main manuscript. The water fraction and concentration of unbranched and branched WLMs in decane were same in Rheo-SANS measurements. After

reaching a steady-state, 2D SANS scattering patterns were collected in the flow-vorticity (1-3) plane of shear as the function of Wi. The 2D images summarized in Figure S4.

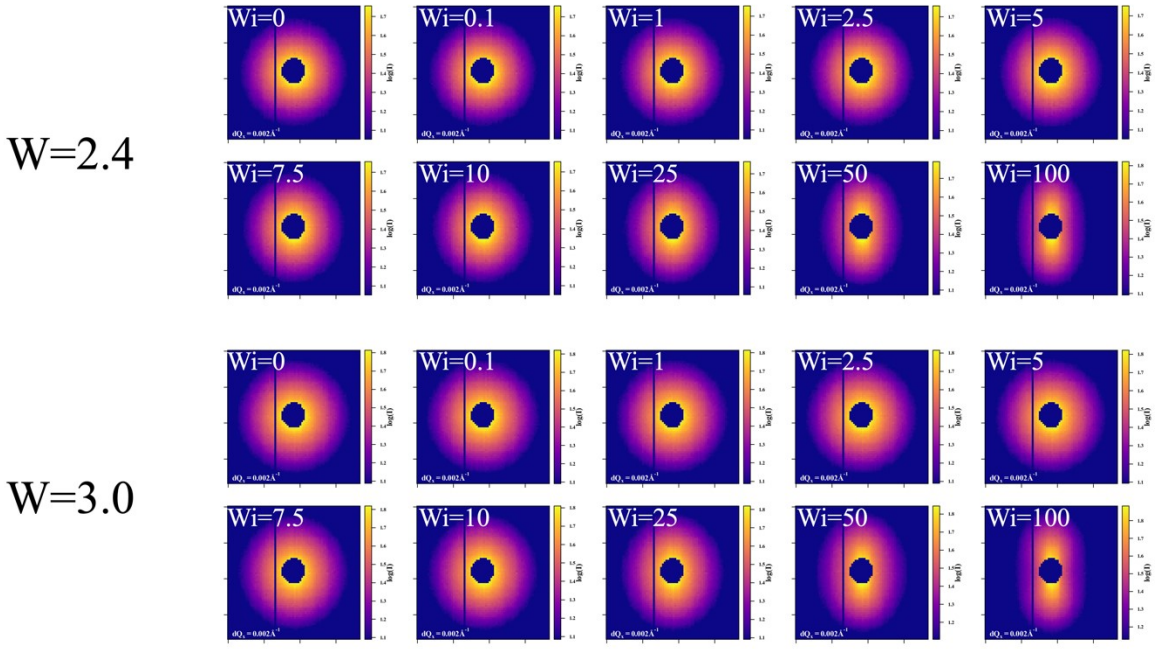

Figure S5. 2D image profiles, annular average, and Q-dependent alignment factors for each Wi between unbranched (W = 2.4) and branched (W = 3.0) WLMs.

S.5. Summary of a sequence of physical processes (SPP) as a function of Wi on both unbranched and branched WLMs.

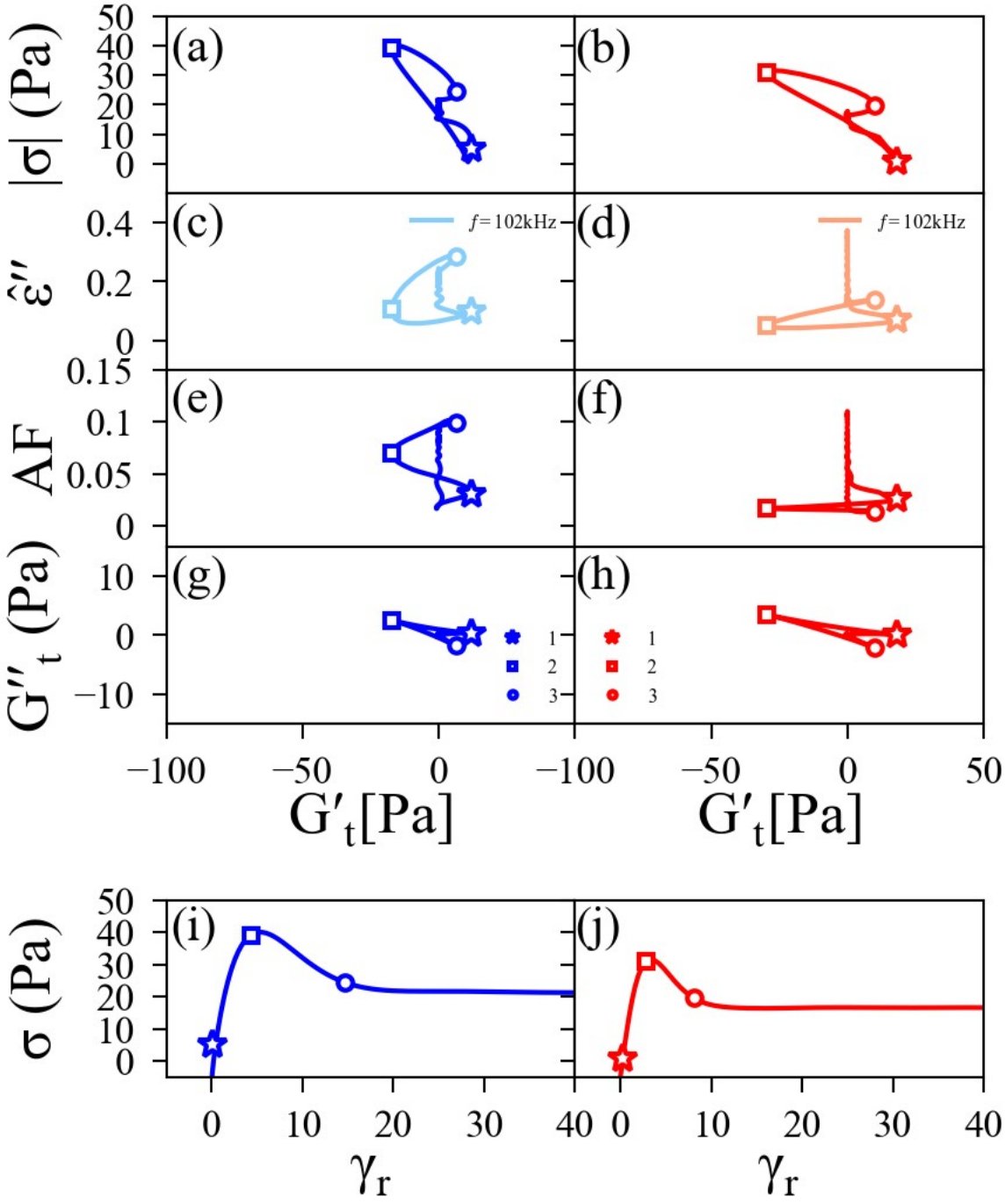

Figure S6. Absolute shear stress, normalized dielectric loss, alignment factor, and transient loss modulus vs. transient storage modulus for unbranched and branched at Wi = 50.

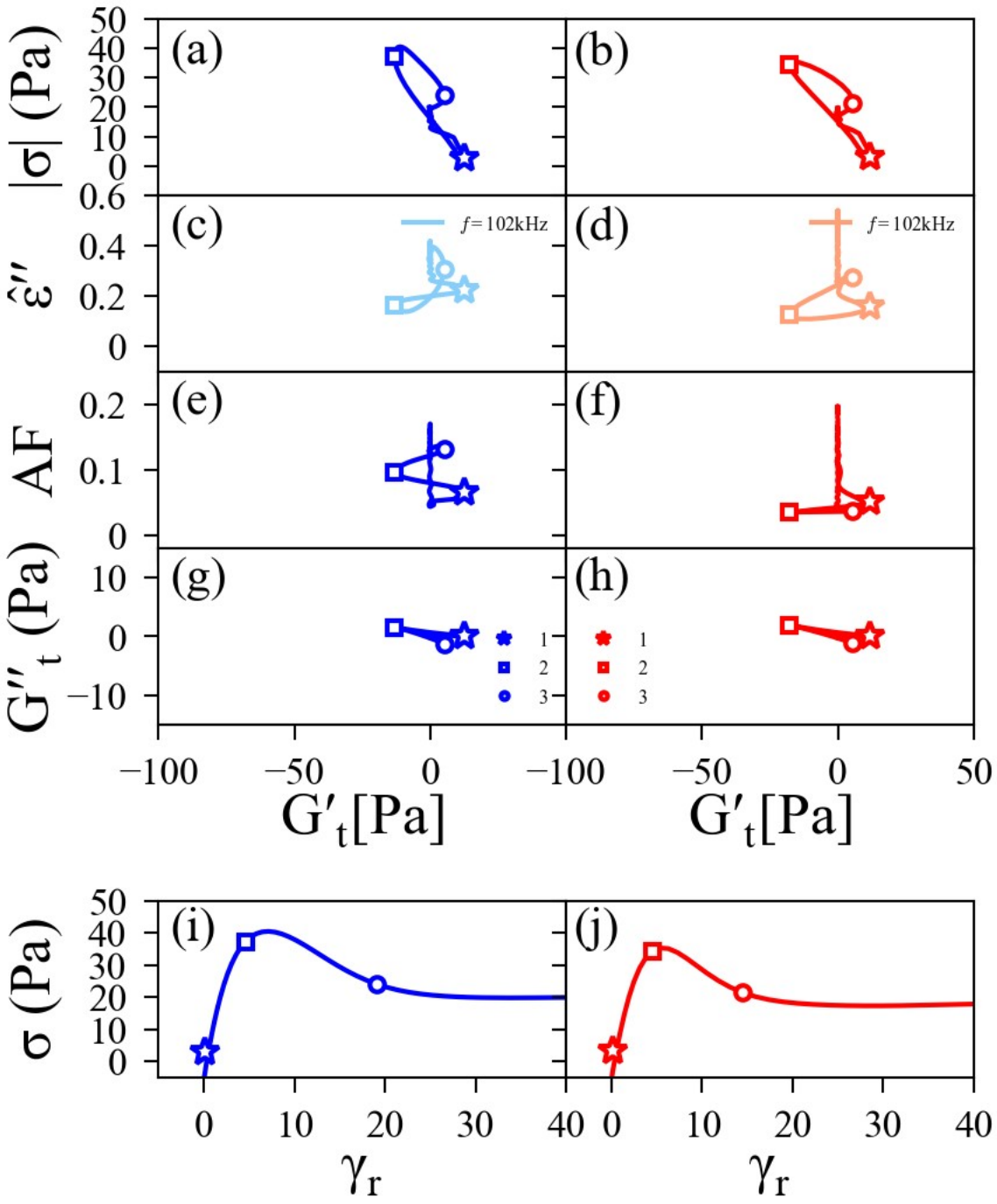

Figure S7. Absolute shear stress, normalized dielectric loss, alignment factor, and transient loss modulus vs. transient storage modulus for unbranched and branched at Wi = 100.